



Heriot-Watt University
Research Gateway

Hydrogel-based reinforcement of 3D bioprinted constructs

Citation for published version:

Melchels, F, Blokzijl, M, Levato, R, Peiffer, Q, De Ruijter, M, Hennink, WE, Vermonden, T & Malda, J 2016, 'Hydrogel-based reinforcement of 3D bioprinted constructs', *Biofabrication*, vol. 8, no. 3, 035004.
<https://doi.org/10.1088/1758-5090/8/3/035004>

Digital Object Identifier (DOI):

[10.1088/1758-5090/8/3/035004](https://doi.org/10.1088/1758-5090/8/3/035004)

Link:

[Link to publication record in Heriot-Watt Research Portal](#)

Document Version:

Peer reviewed version

Published In:

Biofabrication

Publisher Rights Statement:

This is an author-created, un-copyedited version of an article accepted for publication/published in Biofabrication. IOP Publishing Ltd is not responsible for any errors or omissions in this version of the manuscript or any version derived from it. The Version of Record is available online at <http://dx.doi.org/10.1088/1758-5090/8/3/035004>

General rights

Copyright for the publications made accessible via Heriot-Watt Research Portal is retained by the author(s) and / or other copyright owners and it is a condition of accessing these publications that users recognise and abide by the legal requirements associated with these rights.

Take down policy

Heriot-Watt University has made every reasonable effort to ensure that the content in Heriot-Watt Research Portal complies with UK legislation. If you believe that the public display of this file breaches copyright please contact open.access@hw.ac.uk providing details, and we will remove access to the work immediately and investigate your claim.

Hydrogel-based reinforcement of 3D bioprinted constructs

F P W Melchels¹†‡, M M Blokzijl^{1,2}‡, R Levato¹, Q C Peiffer¹,
M de Ruijter¹, W E Hennink², T Vermonden² and J Malda^{2,3}

¹ Department of Orthopaedics, University Medical Center Utrecht, PO Box 85500,
3508 GA Utrecht, The Netherlands

² Department of Pharmaceutics, Utrecht Institute for Pharmaceutical Sciences
(UIPS), Faculty of Science, Utrecht University, PO Box 80082, 3508 TB Utrecht, The
Netherlands

³ Department of Equine Sciences, Faculty of Veterinary Medicine, Utrecht University,
PO Box 80163, 3508 TD Utrecht, The Netherlands

E-mail: j.malda@umcutrecht.nl

Abstract. Progress within the field of biofabrication is hindered by a lack of suitable hydrogel formulations. Here, we present a novel approach based on a hybrid printing technique to create cellularized 3D printed constructs. The hybrid bioprinting strategy combines a reinforcing gel for mechanical support with a bioink to provide a cytocompatible environment. In comparison with thermoplastics such as ϵ -polycaprolactone, the hydrogel-based reinforcing gel platform enables printing at cell-friendly temperatures, targets the bioprinting of softer tissues and allows for improved control over degradation kinetics. We prepared amphiphilic macromonomers based on poloxamer that form hydrolysable, covalently cross-linked polymer networks. Dissolved at a concentration of 28.6%w/w in water, it functions as reinforcing gel, while a 5%w/w gelatin-methacryloyl based gel is utilized as bioink. This strategy allows for the creation of complex structures, where the bioink provides a cytocompatible environment for encapsulated cells. Cell viability of equine chondrocytes encapsulated within printed constructs remained largely unaffected by the printing process. The versatility of the system is further demonstrated by the ability to tune the stiffness of printed constructs between 138 and 263 kPa, as well as to tailor the degradation kinetics of the reinforcing gel from several weeks up to more than a year.

Keywords: Bioprinting, tissue engineering, hydrogel, bioink, mechanical properties

Submitted to: *Biofabrication*

†Present address: Institute of Biological Chemistry, Biophysics and Bioengineering, School of Engineering and Physical Sciences, Heriot-Watt University, Edinburgh, EH14 4AS, United Kingdom

‡These authors contributed equally to this work

1. Introduction

In recent years, 3D bioprinting has emerged as a technology platform showing potential for initiating drastic advances in drug testing, disease models, tissue engineering and regenerative medicine [1]. Bioprinting often employs hydrogels, in this context termed bioinks, in combination with cells to produce complex shapes using 3D printing technologies [2]. Three-dimensional cell culture generally requires hydrogels having low polymer concentrations, low stiffness and low cross-linking densities, to allow unhindered solute diffusion, cell migration and proliferation, as well as deposition of newly formed extracellular matrix [3, 4]. On the other hand, hydrogels for 3D printing with high shape fidelity ideally have high viscosity and yield stress to allow for spatially accurate extrusion, as well as rapid gelation and sufficient mechanical stability to maintain the shape of the final (cross-linked) gel [5].

Particularly for *in vivo* applications, mechanical stability is of utmost importance, and many of the employed bioinks lack sufficient mechanical properties [2]. One promising approach to overcome this hurdle is hybrid printing, in which the functions of mechanical support and cell encapsulation are separated into two materials. Most commonly, a bioink containing cells is co-printed with thermoplastics (ϵ -polycaprolactone in particular) [6, 7, 8, 9, 10, 11], or UV curing adhesive [12]. While effective in improving mechanical properties, these materials either need high temperatures for processing, and/or show poor interaction between hydrophilic and hydrophobic components. Furthermore, they allow limited control over the resulting mechanical properties, and importantly, over degradation kinetics. Particularly for the engineering of mechanically stable soft tissues, no ideal reinforcing material is currently available.

Here, we demonstrate a novel approach for the fabrication of mechanically stable biofabricated constructs, while maintaining control over degradation kinetics and mechanical properties. We aim to achieve this by separating the reinforcing and cell encapsulation functionalities into two distinct hydrogels: one with a high synthetic polymer concentration possessing excellent shape stability upon printing and one with a low natural polymer concentration exhibiting excellent cell encapsulation properties.

2. Materials and methods

2.1. Materials

Poloxamer 407 triblock copolymer (length of the PEG segments equal to 91 repeating units and the PPG segment segment is 56 units long (NMR)). was acquired from BASF (Ludwigshafen, Germany). D,L-lactide, glycolide and L-lactide were purchased from Corbion Purac (Gorinchem, The Netherlands). Irgacure 2959 was obtained from Ciba Specialty Chemicals (Basel, Switzerland). Solvents, unless indicated otherwise, were acquired from Biosolve (Valkenswaard, The Netherlands). Calcein acetoxymethyl ester (calcein-AM), Alamar Blue Cell viability reagent, Dulbecco's Modified Eagle's

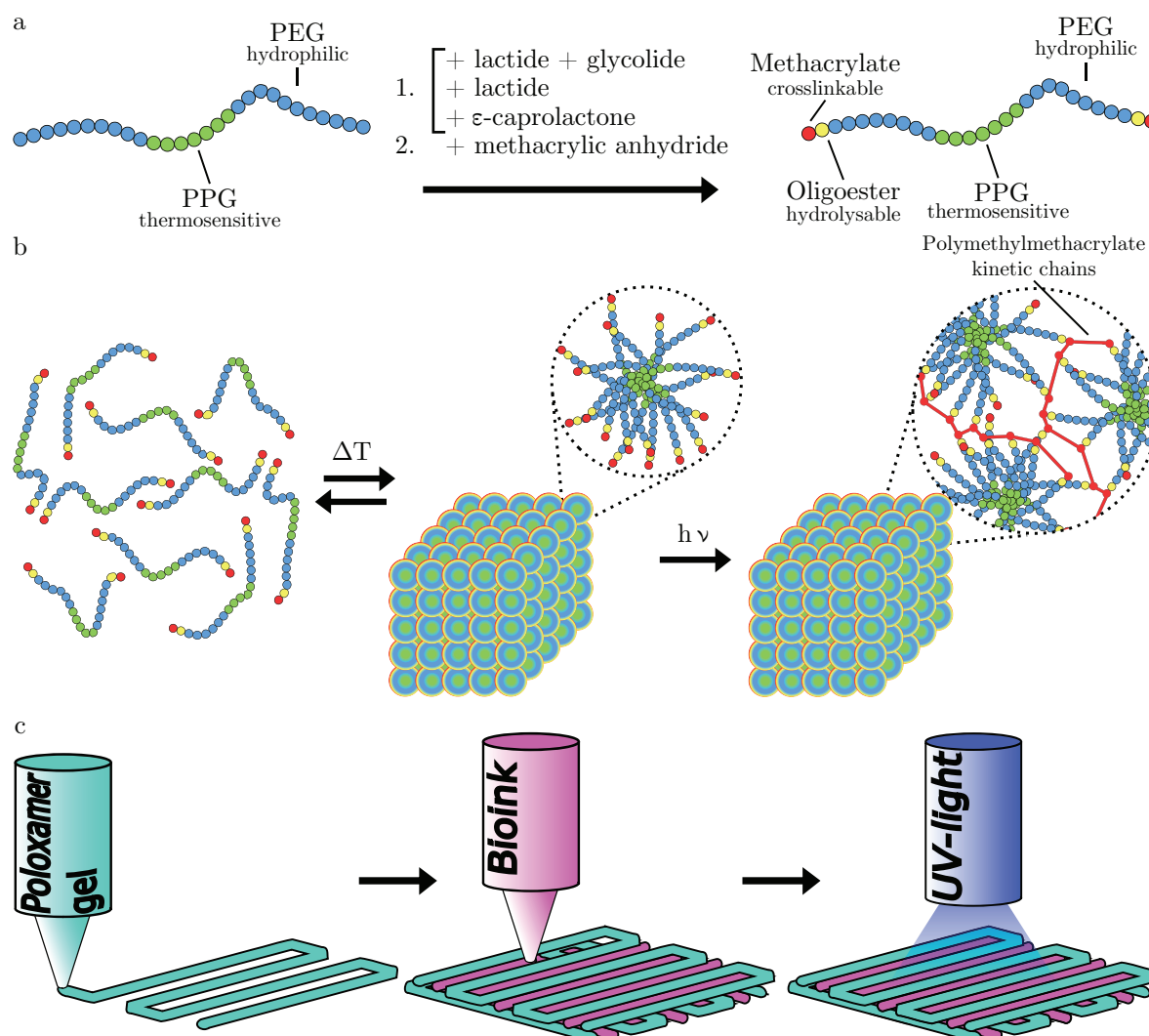


Figure 1. Schematic depictions of a) the modification of poloxamer 407 with oligoesters and methacrylate moieties and b) the temperature-dependent aggregation of modified poloxamer 407 in an aqueous environment. Also shown is the formation of polymethylmethacrylate chains, linking individual macromers together. c) Deposition strategy used to create reinforced gel constructs, with subsequent layers alternating between a 0° and 90° strand orientation.

Medium (DMEM), penicillin, streptomycin and ethidium homodimer were acquired from Fisher Scientific (Landsmeer, The Netherlands). Deuterated chloroform (CDCl_3), ϵ -caprolactone, fluorescein isothiocyanate (FITC), gelatin (type A from porcine skin, 175 g bloom), methacrylic anhydride, sodium azide, stannous octoate ($\text{Sn}(\text{Oct})_2$) and triethylamine (TEA) were all provided by Sigma Aldrich (Zwijndrecht, The Netherlands). Dialysis membranes (Spectra/Por 2, upper molecular weight cutoff 12-14 kDa) were obtained from Carl Roth (Karlsruhe, Germany). Cartridges and extrusion nozzles for 3D printing were obtained from Nordson EFD (Maastricht, The Netherlands). Biopsy punches were acquired from Milltex (Zaventem, Belgium).

All percentages concerning solutions are presented as %w/w, unless stated

otherwise.

2.2. Poloxamer macromers synthesis and characterization

Poloxamer 407 was first dried by azeotropic distillation with toluene using a Dean Stark apparatus and then chain-extended by ring opening polymerization of either ϵ -caprolactone, D,L-lactide, or an equimolar mixture of L-lactide and glycolide for 1 to 2 days at 130 to 150 °C in the presence of $\text{Sn}(\text{Oct})_2$ as a catalyst, under a nitrogen atmosphere. The resulting polymers, and poloxamer 407 itself, were then dissolved in dry dichloromethane at a concentration of 20% and their terminal hydroxyl groups were reacted with a 3 times excess of methacrylic anhydride in the presence of an amount of triethylamine equal to the amount of methacrylic anhydride added. During the reaction, samples were taken and their NMR spectra were recorded in CDCl_3 . When insufficient conversion was observed, another 3 times excess methacrylic anhydride and an equimolar amount of triethylamine were added to the reaction mixture. Purification was realized by precipitation from diethyl ether and drying under ambient conditions. The resulting macromonomers (macromers) are abbreviated as P-CL-MA, P-LA-MA and P-LG-MA, with ϵ -caprolactone, D,L-lactide or an L-lactide-*co*-glycolide oligoesters, respectively. The macromer not possessing any hydrolysable ester will be referred to as P-MA. The targeted block lengths for the terminal ester blocks were 1 repeating unit for caprolactone, 2 for D,L-lactide and a combined total of 4 for L-lactide-*co*-glycolide. Poloxamer macromers were analyzed using ^1H NMR (Varian 400 MHz), with samples dissolved in CDCl_3 . More detailed information on macromer composition, analysis and acronyms is available in the supporting info.

2.3. Gelatin methacryloyl synthesis and characterization

GelMA was synthesized by reacting gelatin with methacrylic anhydride, as reported previously [13]. FITC-labeled gelMA was created by reacting FITC with gelMA in a 0.1 M NaHCO_3 buffer at a pH of 9. For purposes of illustration, FITC-labeled gelMA was then used to create images of samples where it would otherwise be difficult to discriminate between poloxamer gel and gelMA.

2.4. Rheological characterization

Reinforcing gels were prepared by dissolving modified and unmodified poloxamer 407 at 28.6% in PBS. Their flow behavior was analyzed using a DHR2 rheometer (TA Instruments, Etten-Leur, The Netherlands), equipped with a Peltier plate and 40 mm cone at a truncation gap of 54 μm . Viscosity as a function of temperature was measured by heating the plate from 4 to 25 °C at a rate of 5 °C min^{-1} . A shear rate of 100 s^{-1} was applied to approximate the shear rate experienced by gels in the nozzle of a 3D printer. Yield shear stress was measured by gradually increasing the torque from 0 to beyond the point where flow was observed. The stress value assigned to the yield stress

was calculated by determining the peak value of the derivative of viscosity versus stress. Shear thinning behavior was measured by recording the viscosity as a function of shear rate from 0.003 to 1000 s⁻¹ at a temperature of 21 °C.

2.5. Construction of reinforced 3D printed gels

The reinforcing gel was prepared by adding P-MA to PBS at a concentration of 28.6% and was subsequently dissolved over 36 hours at 4 °C. GelMA was dissolved at a concentration of 5% in PBS at 37 °C for one hour. Both gel-precursors were supplemented with 0.1% Irgacure 2959.

CAD-models of various anatomical objects were translated into g-code using MMconverter (regenHU, Villaz-St-Pierre, Switzerland), applying a layer height of 0.24 mm and a strand spacing of 1.8 mm. **Strand spacing indicates the distance between the midpoints of adjacent strands in the horizontal plane.** Alternatively, samples for the analysis of printed construct stiffness were created by manually drawing the printer path in vector graphics and translating this into g-code using BioCAD (regenHU, Villaz-St-Pierre, Switzerland). **Layer height was set at 0.24 mm and a total height of 2.16 or 0.96 mm was used for samples for mechanical testing and cytocompatibility tests, respectively.** In both cases, the produced g-code can be read and executed on a 3DDiscovery bioprinter (regenHU, Villaz-St-Pierre, Switzerland). The bioprinter was provided with two cartridges. One was filled with the reinforcing gel and the other filled with the bioink. Print cartridges were kept at room temperature and 37 °C, respectively. Extrusion was air-pressure driven and for the reinforcing gel its pressure was set at 1.2 bar and 0.5 bar for the gelMA gel. Conical nozzles (27G) were used for deposition of reinforcing gel, whereas gelMA gels were deposited using a temperature controlled microvalve and nozzle (regenHU, Villaz-St-Pierre, Switzerland), with an inner diameter of 0.3 mm. Each deposited layer was illuminated for 10 seconds using a built-in UV-led ($\lambda = 365$ nm, $E = 240.2$ mW cm⁻² at $h = 1$ cm) and completely built samples were subjected to an additional 15 minutes post cross-linking using a Vilber Lourmat portable UV-lamp ($\lambda = 365$ nm, $E = 3$ mW cm⁻² at $h = 2$ cm) (Hartenstein, Würzburg, Germany).

Different strand distances were used to create samples with varying weight ratios of P-MA reinforcing gel to gelMA bioink. The stiffness of these constructs was subsequently measured as described below in section 2.7.

2.6. Hydrolytic degradation of reinforcing gels

Macromers P-MA, P-CL-MA, P-LA-MA, P-LG-MA as well as a 1:1 mixture of P-LA-MA and P-CL-MA were dissolved in PBS at a concentration of 28.6% with 0.1% Irgacure 2959. Gel precursor solutions were obtained after 36 hours of dissolution at 4 °C, these were injected into molds and subsequently cross-linked using a UV cross-linker (CL-1000, $\lambda = 365$ nm, 10.9 mW cm⁻² at $h = 6$ cm) (UVP, Cambridge, United Kingdom) for 15 minutes to yield disks with a diameter and height of 6 and 2 mm, respectively.

To study degradation, gels were placed in 50 ml PBS supplemented with 0.02% sodium azide to prevent bacterial growth and stored at 37 °C.

2.7. Mechanical characterization

Printed gel squares were cut to similar size as the molded gels using a 6 mm diameter biopsy punch. Both printed and cast samples were then subjected to uniaxial, unconfined compression at a strain rate of 30% min⁻¹ between two parallel plates using a Q800 dynamical mechanical analyzer (TA Instruments, Etten-Leur, The Netherlands), up to 20% strain. Stiffness of the printed samples and Youngs modulus of the cast gels was calculated from the slope of the stress-strain curve between 3 and 10% strain.

2.8. Cell viability

Equine chondrocytes were isolated from the metacarpal joint of a deceased healthy adult donor, age 5 years. Cells at passage 1 were suspended at a concentration of $1 \cdot 10^6$ cells ml⁻¹ in a 5% gelMA solution with 0.1% Irgacure 2959 in PBS at 37 °C. This cell-containing bioink was then printed four layers high, with either 28.6% P-MA or P-LG-MA based hydrogels as reinforcing material and using similar settings as those used to obtain samples for tuning the stiffness.

Printed samples containing encapsulated cells were cultured for up to 14 days in DMEM supplemented with 10% fetal calf serum and 1% penicillin/streptomycin. Assessment of cell viability was performed at day 1, 7 and 14 using calcein-AM and ethidium homodimer to label living and dead cells, respectively. Samples were incubated for 15 minutes in Dulbecco PBS supplemented with 25 μ M calcein-AM and 2 μ M ethidium homodimer. From each sample three pictures were taken using an IX53 microscope with XC50 camera (Olympus, Zoeterwoude, The Netherlands) and cells labeled red or green were counted using ImageJ software.

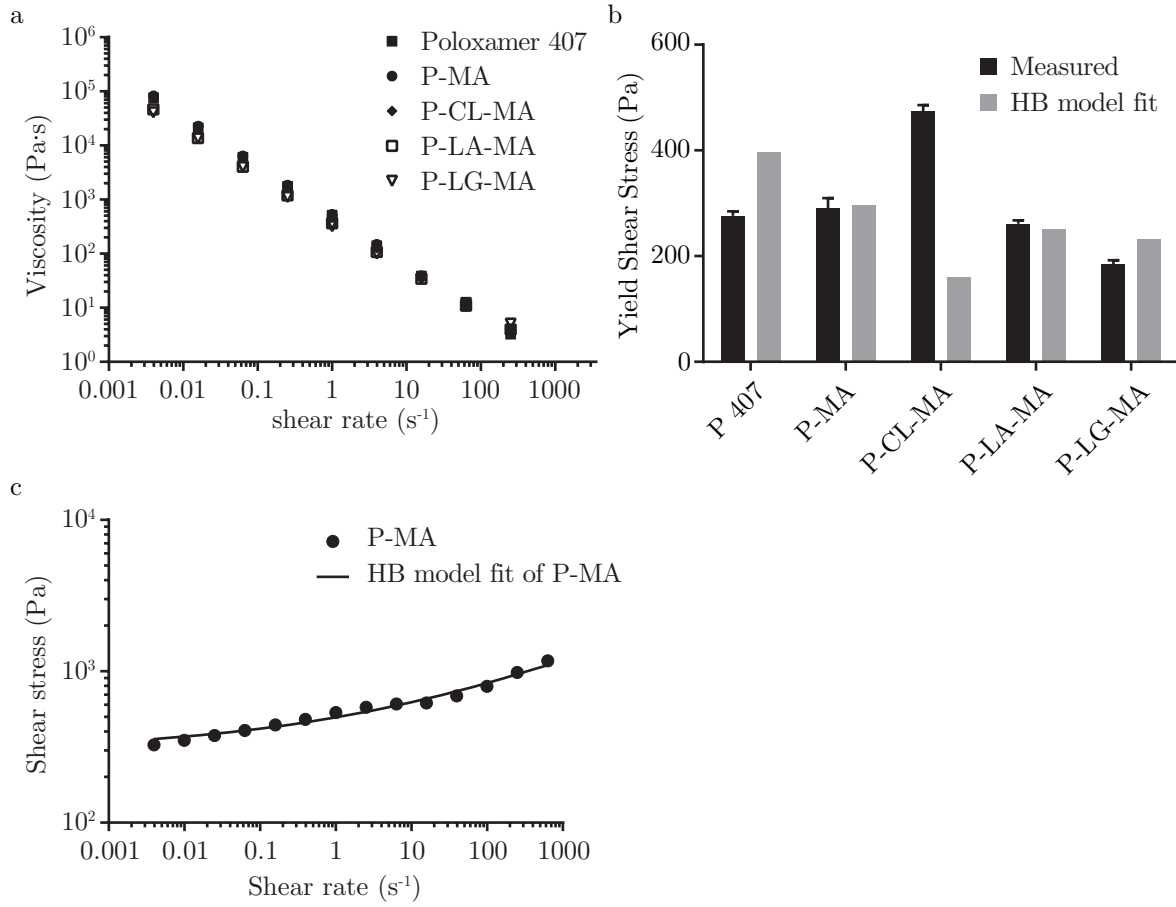
Metabolic activity of cells encapsulated in printed constructs was evaluated using the Alamar Blue reagent at day 1, 3, 7 and 14. For analysis, samples were incubated for four hours with DMEM supplemented with 10% Alamar Blue. The supernatant media was collected and analyzed on a Fluoroskan Ascent FL microplate reader (Thermo Scientific, Breda, The Netherlands) using an excitation and detection wavelength of 470 nm and 590 nm, respectively. Fluorescence intensity was compared against a calibration curve composed of known chondrocyte numbers.

2.9. Statistical methods

Each experiment was performed in three to six replicates ($n = 3$ - $n = 6$). Data are presented as mean and standard deviation of the replicates. A student's t-test was applied assuming Gaussian distribution of the data and p-values lower than 0.05 were considered as significantly different.

Table 1. Herschel-Bulkley fitting parameters applied to shear stress over rate data obtained from shear rate sweeps. With consistency index K and flow index n .

	K (Pa.s)	n (-)	R^2
P 407	44.7	0.45	0.96
P-MA	199.2	0.22	0.98
P-CL-MA	315.2	0.11	0.92
P-LA-MA	66.6	0.47	0.99
P-LG-MA	83.0	0.46	0.99

**Figure 2.** a) Shear thinning behavior of reinforcing gels, b) directly measured yield shear stress for the four reinforcing gels and unmodified poloxamer gel compared against extrapolated yield stress from the Herschel-Bulkley model and c) fit of Herschel-Bulkley model to shear stress over rate data.

3. Results & Discussion

3.1. Poloxamer macromer synthesis and characterization

Building on previous work [14], we have developed printable hydrogels based on modified poloxamer 407. Poloxamer 407 was selected for modification because hydrogels based on poloxamer present excellent properties for 3D printing [14, 15, 16]. These triblock

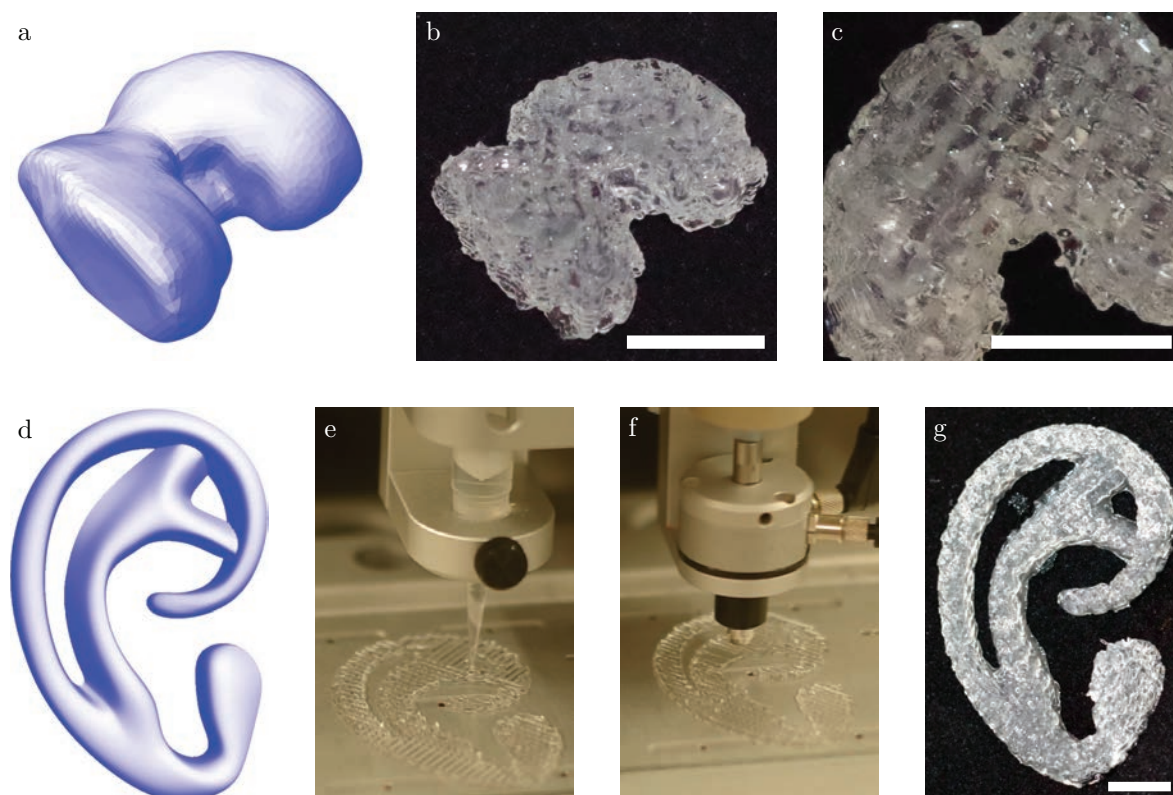


Figure 3. a) Render of a CAD file corresponding to a femoral condyle, b) Femoral condyle, 3D printed from reinforcing gel and bioink, and c) bottom-view of printed femoral condyle, showing gelMA strands (opaque) and poloxamer strands (transparent). d) Render obtained from CAD file corresponding to the auricular cartilage. e-f) Action of the print heads depositing reinforcing gel and bioink, respectively. g) Model of auricular cartilage, as printed using hybrid printing. Scale-bars indicate 10 mm.

copolymers were chain-extended with α -hydroxy acids and methacrylate moieties, yielding 3 different hydrolysable macromonomers. Additionally, a non-degradable variant was also synthesized that does not possess an oligoester spacer. In aqueous environments, these macromers exhibit a lower critical solution temperature (LCST). At temperatures below the LCST, the PPG segments are hydrated, while at elevated temperatures they dehydrate and aggregate, resulting in the entropy-driven formation of micelles. Above the critical aggregation concentration (CAC) and LCST, the PEG coronas start to overlap and entangle, resulting in the formation of a highly viscous physical gel [17]. Modified poloxamer 407 gels exhibit shear thinning behavior when the imposed shear stress exceeds the yield shear stress, as occurs in the nozzle of a 3D printer [13]. We selected a reinforcing gel concentration of 28.6% (0.4 g per ml solvent), which is above the CAC [17] and was found to be sufficient for 3D printing application, while yielding stiff gels with rubber-like appearance after cross-linking under ambient conditions.

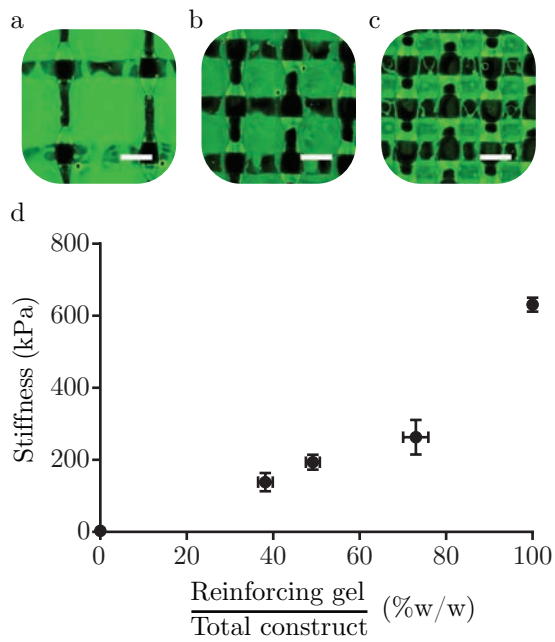


Figure 4. a), b), c) Fluorescence microscopy pictures corresponding to hybrid printed structures with strand distances of 2.7, 1.8 and 1.35 mm, respectively. GelMA is shown green, whereas P-MA reinforcing gel is unstained and appears dark. Scale bars indicate 1 mm. d) Stiffness as a function of the weight percentage of reinforcing gel deposited to create hybrid 3D printed structures. A strand spacing of 2.7, 1.8 and 1.35 mm was used to produce gels with a weight ratio of reinforcing gel of 38.2 ± 1.7 , 49.2 ± 1.6 and 73.0 ± 2.9 %w/w, respectively. The stiffness of cast 5% gelMA and 28.6% P-MA gel disks is included for comparison and for 5% gelMA this is equal to 2.7 kPa.

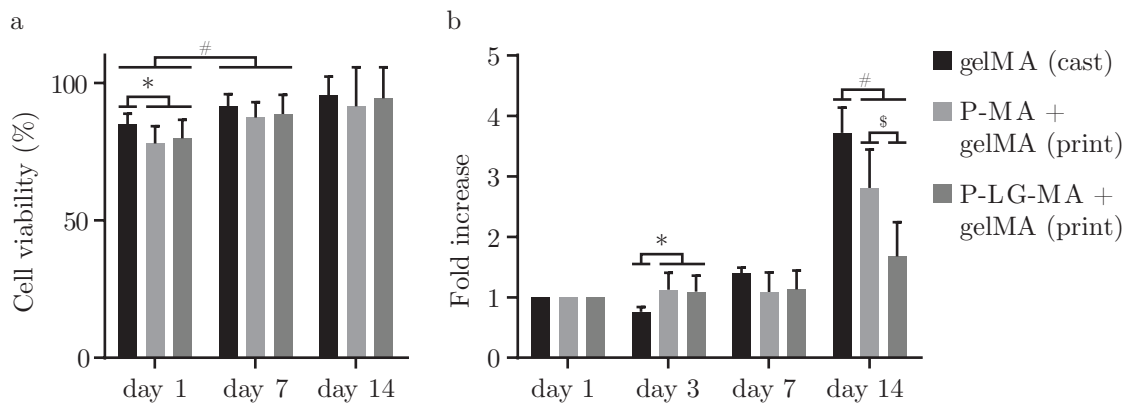


Figure 5. a) Cell viability within the bioink of printed P-MA reinforced constructs at day 1, 7 and 14, compared to cell viability within cast gelMA gels. b) Metabolic activity of equine chondrocytes, normalized to the activity day 1 for each condition at day 1, 3, 7 and 14.

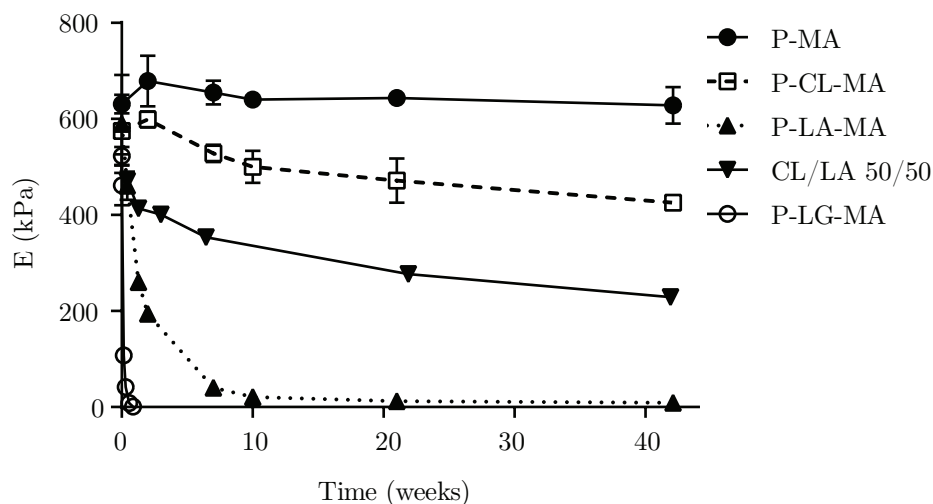


Figure 6. Youngs modulus of reinforcing gels after being submerged in PBS at 37 °C, measured over time. Also shown is a gel crosslinked from a 50/50 mixture of P-CL-MA and P-LA-MA macromers.

3.2. Rheological characterization

The modified poloxamer-based hydrogels exhibit a nearly identical rheological behavior when compared to gels based on unmodified poloxamer. Two rheological phenomena critical to suitability for 3D printing are observed to a similar extent in all gels, being shear thinning and yield stress, as shown in figure 2a and figure 2b, respectively. The Herschel-Bulkley model, which combines these two properties of non-Newtonian fluid behavior, was fitted to flow sweep data for all gels with high correlation as demonstrated in figure 2c and table 1. Values of n much smaller than unity confirm the shear thinning effect, while yield stresses of several hundred Pa are sufficient to prevent sagging of printed structures. The yield stress derived from the Herschel-Bulkley model represents residual stress that remains when extrapolating to zero shear rate. Therefore, its value is sensitive to the range of data points selected for fitting; for all gels we used 28 data points in the same range (4^{-3} to 1000 s^{-1}), at logarithmic intervals.

In addition, we directly measured yield stress for each gel by slowly increasing torque on a static gel in the rheometer. The yield point is defined as the first point at which a strain can be measured. This indicates initiation of flow, and it is followed by a large drop in viscosity upon further increase in torque. Directly measured yield stress is highly reproducible, with values being in the same order of magnitude as fitted values (figure 2b).

The higher yield stress observed for P-CL-MA based gels could originate from the higher hydrophobicity of caprolactone, thus exhibiting a stronger interaction with the hydrophobic PPG domains when compared to the three other macromers, which are slightly more hydrophilic. This effect has actually been exploited to achieve more stable poloxamer-based micelles previously [18].

Temperature sweeps (figure S2 in Supplementary Information) showed 1 - 5 °C

shifts upwards for the LCST value of modified poloxamers as compared to unmodified poloxamer (LCST = 12 °C). Although the thermosensitivity is not directly exploited in the ambient printing process (other than facilitating loading of cartridges using cold solutions), it further confirms that the oligoester and methacrylate modification has had limited effect on the rheological behavior of highly printable poloxamer 407 based hydrogels.

3.3. Construction of reinforced 3D printed gels

As can be seen from figure 3, the hybrid 3D bioprinting approach proposed allows for the generation of complex shapes. Here, the reinforcing gel strands were found to be 0.3 mm wide. The selected bioink was composed of 5% gelatin methacryloyl (gelMA), for its desirable properties for cell encapsulation [19, 20, 21, 22]. Previously, 3D printing of bioinks based on 10% gelMA was realized by addition of viscosity or gelation modifiers [13, 23], or by strictly controlling temperature [20]. Here, a gelMA bioink with a concentration as low as 5% was deposited in-between strands of P-MA reinforcing gel, building a 3D construct up 10 mm high. To demonstrate the improved control over printed geometry, also a more challenging shape was produced, resembling the auricular cartilage.

This hybrid bioprinting approach allows control over the mechanical properties of the construct within a specific range, by altering the composition of the 3D print. Specifically, this can be achieved by increasing or decreasing the distance between adjacent strands of the reinforcing gel, thus influencing the weight ratio of reinforcing gel with respect to the bioink in the printed construct. This approach resulted in the ability to tailor the overall stiffness of printed gel constructs. For instance, a strand spacing of 2.7 mm yielded a stiffness of 138 ± 25 kPa, while decreasing this distance to 1.35 mm increased the overall stiffness about two fold to 263 ± 48 kPa, as can be seen from figure 4. The achieved stiffness demonstrated here is considerably lower than that of samples reinforced using thermoplastics such as polycaprolactone, which exhibit stiffness values up to several MPa [9, 24]. For this reason, reinforcing gels may be particularly advantageous for the bioprinting of soft tissues, for which currently very few options for reinforcing exist.

3.4. Cell viability and metabolic activity

To demonstrate the cytocompatibility of this hybrid bioprinting approach, equine chondrocytes embedded within a 5% gelMA gel were co-printed with P-MA or P-LG-MA reinforcing gel into a hybrid construct. When compared to cells encapsulated in the cast gelMA control, viability did only differ significantly on the first day after printing, as represented in figure 5a. On days 7 and 14 viability was similar for all three groups and passed the 90% mark on day 14. Cell viability after two weeks remains largely unaffected by the hybrid printing approach.

On the other hand, metabolic activity, as shown in figure 5b shows a more pronounced difference between the three groups, especially at day 14. Even so, it should be noted that an increase of metabolic activity may be observed over time. Lower metabolic activity found for hybrid scaffolds using P-LG-MA based reinforcing gels could be explained by a loss of structural integrity due to rapid degradation of the reinforcing component. Our data suggests that cells inside the gelMA component of the hybrid printed scaffolds survive and proliferate. Even though free poloxamer above a critical concentration could be harmful to cells [25], it is unlikely that these concentrations are achieved in culture using the hybrid printing approach in combination with fast degrading modified poloxamer-based gels.

3.5. Hydrolytic degradation of reinforcing gels

Regenerative approaches aim to fully restore the tissue which means that over time, the implanted material should be cleared from the body and its function taken over by newly formed tissue [26]. This requires a precise control over the timing and mechanism of scaffold degradation. However, not all currently investigated printable biomaterials allow fine-tuning of their degradation kinetics. Because of the flexibility of the modified poloxamer macromer platform, a broad range of degradation rates could be realized. Based on a principle first demonstrated by Hubbell in 1993 for poly(ethylene glycol) based hydrogels, incorporation of a degradable oligoester spacer between poloxamer and methacrylate moiety allows degradation of cross-linked hydrogels obtained from these macromers to be tuned as desired [27]. Considering figure 6 it can be seen that upon incubation in PBS at 37 °C, gel disks prepared from P-LG-MA macromers show a rapid decline in stiffness within the first week and fully dissociate within 2 weeks. On the contrary, P-CL-MA gels exhibit limited loss of structural integrity even after 40 weeks. Since poloxamer-oligoester based gels degrade via bulk degradation, mass loss of the hydrated gel is negligible up to the point where no covalent crosslinks remain. Beyond this point, gels disintegrate and dissolve rapidly [28]. All gels tested in this study, except those composed of P-MA, show a decline in Young's modulus over time.

4. Conclusion

In order for a biofabrication strategy to be successful, it should fulfill both biological and mechanical aspects to an optimal extent. We have presented here a novel approach that can contribute towards the bioprinting of mechanically stable soft tissues, by separating these two functions into two different and specialized hydrogels. This has resulted in a strategy that allows for accurate control over mechanical properties and degradation kinetics. Finally, we would like to highlight the potential of this technique by mentioning it may also find application in other areas of research currently utilizing hydrogels, such as soft robotics [29], biosensors [30, 31] and artificial organs [32, 1], but foremost in tissue engineering, where it may contribute to the manufacturing of implantable, mechanically

stable functional tissues.

Acknowledgments

We kindly acknowledge Iris Otto for providing us with a CAD model of the auricular cartilage. Research leading to this work has received funding from the Dutch Arthritis Foundation (LLP-12); the European Community's Seventh Framework Programme (FP7/2007-2013) under grant agreement 309962 (HydroZONES); and the European Research Council under grant agreement 647426 (3D-JOINT).

References

- [1] Sean V Murphy and Anthony Atala. 3D bioprinting of tissues and organs. *Nature Biotechnology*, 32(8):773–785, aug 2014.
- [2] Jos Malda, Jetze Visser, Ferry P W Melchels, Tomasz Jüngst, Wim E Hennink, Wouter J A Dhert, Jürgen Groll, and Dietmar W Hutmacher. 25th Anniversary Article: Engineering Hydrogels for Biofabrication. *Advanced Materials*, 25(36):5011–5028, sep 2013.
- [3] Cole A DeForest and Kristi S Anseth. Advances in Bioactive Hydrogels to Probe and Direct Cell Fate. *Annual Review of Chemical and Biomolecular Engineering*, 3:421–444, 2012.
- [4] Dror Slikkard. Designing Cell-Compatible Hydrogels for Biomedical Applications. *Science*, 336(2012):1124–1128, 2012.
- [5] Tomasz Jungst, Willi Smolan, Kristin Schacht, Thomas Scheibel, and Jürgen Groll. Strategies and Molecular Design Criteria for 3D Printable Hydrogels. *Chemical Reviews*, oct 2015.
- [6] Kristel W M Boere, Jetze Visser, Hajar Seyednejad, Sima Rahimian, Debby Gawlitta, Mies J van Steenbergen, Wouter J A Dhert, Wim E Hennink, Tina Vermonden, and Jos Malda. Covalent attachment of a three-dimensionally printed thermoplast to a gelatin hydrogel for mechanically enhanced cartilage constructs. *Acta Biomaterialia*, 10(6):2602–2611, 2014.
- [7] Falguni Pati, Jinah Jang, Dong Heon Ha, Sung Won Kim, Jong Won Rhie, Jin Hyung Shim, Deok Ho Kim, and Dong Woo Cho. Printing three-dimensional tissue analogues with decellularized extracellular matrix bioink. *Nature Communications*, 5:1–11, jun 2014.
- [8] Falguni Pati, Dong Heon Ha, Jinah Jang, Hyun Ho Han, Jong Won Rhie, and Dong Woo Cho. Biomimetic 3D tissue printing for soft tissue regeneration. *Biomaterials*, 62:164–175, sep 2015.
- [9] Wouter Schuurman, V Khristov, Michiel W Pot, P René van Weeren, Wouter J A Dhert, and Jos Malda. Bioprinting of hybrid tissue constructs with tailorable mechanical properties. *Biofabrication*, 3(2):021001, jun 2011.
- [10] Jin Hyung Shim, Jong Young Kim, Min Park, Jaesung Park, and Dong Woo Cho. Development of a hybrid scaffold with synthetic biomaterials and hydrogel using solid freeform fabrication technology. *Biofabrication*, 3(3):034102, sep 2011.
- [11] Jetze Visser, Benjamin Peters, Thijs J Burger, Jelle Boomstra, Wouter J A Dhert, Ferry P W Melchels, and Jos Malda. Biofabrication of multi-material anatomically shaped tissue constructs. *Biofabrication*, 5(3):035007, sep 2013.
- [12] Shannon E Bakarich, Robert Gorkin, Marc in het Panhuis, and Geoffrey M Spinks. Three-Dimensional Printing Fiber Reinforced Hydrogel Composites. *ACS Applied Materials & Interfaces*, 6(18):15998–16006, sep 2014.
- [13] Ferry P W Melchels, Wouter J A Dhert, Dietmar W Hutmacher, and Jos Malda. Development and characterisation of a new bioink for additive tissue manufacturing. *Journal of Materials Chemistry B*, 2(16):2282, 2014.
- [14] Natalja E Fedorovich, Ives Swennen, Jordi Girones, Lorenzo Moroni, Clemens A van Blitterswijk,

- Etienne Schacht, Jacqueline Alblas, and Wouter J A Dhert. Evaluation of photocrosslinked Lutrol hydrogel for tissue printing applications. *Biomacromolecules*, 10(7):1689–96, jul 2009.
- [15] Michael Müller, Jana Becher, Matthias Schnabelrauch, and Marcy Zenobi-Wong. Nanostructured Pluronic hydrogels as bioinks for 3D bioprinting. *Biofabrication*, 7(3):035006, aug 2015.
- [16] David B Kolesky, Ryan L Truby, A Sydney Gladman, Travis A Busbee, Kimberly A Homan, and Jennifer A Lewis. 3D bioprinting of vascularized, heterogeneous cell-laden tissue constructs. *Advanced Materials*, 26(19):3124–3130, feb 2014.
- [17] Vincent Lenaerts, Caroline Triqueneaux, Michel Quartern, Françoise Rieg-Falson, and Patrick Couvreur. Temperature-dependent rheological behavior of Pluronic F-127 aqueous solutions. *International Journal of Pharmaceutics*, 39(1-2):121–127, 1987.
- [18] Yan Zhang, Li Zhao, Min Chen, and Meidong Lang. Synthesis and properties of Pluronic-based pentablock copolymers with pendant amino groups. *Colloid and Polymer Science*, 291(7):1563–1571, jul 2013.
- [19] Hug Aubin, Jason W Nichol, Ché B Hutson, Hojae Bae, Alisha L Sieminski, Donald M Crokek, Payam Akhyari, and Ali Khademhosseini. Directed 3D cell alignment and elongation in microengineered hydrogels. *Biomaterials*, 31(27):6941–6951, sep 2010.
- [20] Thomas Billiet, Elien Gevaert, Thomas De Schryver, Maria Cornelissen, and Peter Dubruel. The 3D printing of gelatin methacrylamide cell-laden tissue-engineered constructs with high cell viability. *Biomaterials*, 35(1):49–62, jan 2014.
- [21] Ying Chieh Chen, Ruei Zeng Lin, Hao Qi, Yunzhi Yang, Hojae Bae, Juan M Melero-Martin, and Ali Khademhosseini. Functional human vascular network generated in photocrosslinkable gelatin methacrylate hydrogels. *Advanced Functional Materials*, 22(10):2027–2039, may 2012.
- [22] Jason W Nichol, Sandeep T Koshy, Hojae Bae, Chang M Hwang, Seda Yamanlar, and Ali Khademhosseini. Cell-laden microengineered gelatin methacrylate hydrogels. *Biomaterials*, 31(21):5536–5544, jul 2010.
- [23] Wouter Schuurman, Peter A Levett, Michiel W Pot, Paul René van Weeren, Wouter J A Dhert, Dietmar W Hutmacher, Ferry P W Melchels, Travis J Klein, and Jos Malda. Gelatin-Methacrylamide Hydrogels as Potential Biomaterials for Fabrication of Tissue-Engineered Cartilage Constructs. *Macromolecular Bioscience*, 13(5):551–561, may 2013.
- [24] Jetze Visser, Ferry P W Melchels, June E Jeon, Erik M van Bussel, Laura S Kimpton, Helen M Byrne, Wouter J A Dhert, Paul D Dalton, Dietmar W Hutmacher, and Jos Malda. Reinforcement of hydrogels using three-dimensionally printed microfibres. *Nature Communications*, 6:6933, apr 2015.
- [25] Sarwat F Khattak, Surita R Bhatia, and Susan C Roberts. Pluronic F127 as a Cell Encapsulation Material: Utilization of Membrane-Stabilizing Agents. *Tissue Engineering*, 11(5-6):974–983, may 2005.
- [26] Dietmar W Hutmacher. Scaffolds in tissue engineering bone and cartilage. *Biomaterials*, 21(24):2529–2543, dec 2000.
- [27] Amarpreet S Sawhney, Chandrashekhar P Pathak, and Jeffrey A Hubbell. Bioerodible hydrogels based on photopolymerized poly(ethylene glycol)-co-poly(α -hydroxy acid) diacrylate macromers. *Macromolecules*, 26(4):581–587, jul 1993.
- [28] Andrew T Metters, Christopher N Bowman, and Kristi S Anseth. A Statistical Kinetic Model for the Bulk Degradation of PLA- b -PEG- b -PLA Hydrogel Networks. *The Journal of Physical Chemistry B*, 104(30):7043–7049, aug 2000.
- [29] Sangbae Kim, Cecilia Laschi, and Barry Trimmer. Soft robotics: a bioinspired evolution in robotics. *Trends in Biotechnology*, 31(5):287–294, may 2013.
- [30] Sanlin S Robinson, Kevin W OBrien, Huichan Zhao, Bryan N Peele, Chris M Larson, Benjamin C Mac Murray, Ilse M van Meerbeek, Simon N Dunham, and Robert F Shepherd. Integrated soft sensors and elastomeric actuators for tactile machines with kinesthetic sense. *Extreme Mechanics Letters*, 2015.
- [31] Kiyoshi Sawahata, Jian Ping Gong, and Yoshihito Osada. Soft and wet touch-sensing system

- 408 made of hydrogel. *Macromolecular Rapid Communications*, 16(10):713–716, oct 1995.
- 409 [32] Ferry P W Melchels, Marco A N Domingos, Travis J Klein, Jos Malda, Paulo J Bartolo, and
- 410 Dietmar W Hutmacher. Additive manufacturing of tissues and organs. *Progress in Polymer*
- 411 *Science*, 37(8):1079–1104, 2012.

Supporting information

NMR spectroscopy

Poloxamer 407 macromonomers were dissolved in deuterated chloroform and their ^1H NMR spectra recorded on a Varian 400 MHz NMR spectrometer. From the resulting spectra, shown in figure S1, oligomerization of α -hydroxy acids and conversion of hydroxyl to methacrylate were quantified by comparing oligoester and methacrylate proton peaks to PEG and PPG peaks. The integral at 4.29 ppm was assigned a value of 4, corresponding to the 4 protons at the terminal esters of each chain. The number of caprolactone monomers, lactide dimers and glycolide dimers per polymer chain was subsequently calculated according to (1), (2) and (3), respectively. Equation (4) was used to calculate conversion of hydroxyl moieties to methacrylates. In each equation, I_x denotes the value of integral I at a ppm value of x .

$$P_{CL} = \frac{I_{1.22-1.85}}{10} \quad (1)$$

$$P_{LA} = \frac{I_{1.57} + 3 \cdot I_{5.15}}{24} \quad (2)$$

$$P_{LG} = \frac{I_{4.7}}{4} \quad (3)$$

$$DM = \frac{I_{1.96} + 3 \cdot I_{5.57} + 3 \cdot I_{6.13}}{18} \quad (4)$$

Degrees of polymerization observed for the chain-extended poloxamers were found to be less than 2 repeating units per polymer chain end for P-CL-MA and P-LA-MA. For P-LG-MA up to 2 repeating units were present per polymer chain end as shown in table S1. More than 91% conversion of hydroxyl end groups to methacrylates was observed for all the four different macromers.

Table S1. List of the 4 different macromers, the type of lactone and their corresponding feed ratios.

Name	Lactone	Feed ^a	Block Length ^a	Feed MA ^b	Conversion ^c
P-MA	-	-	-	4	95%
P-CL-MA	ϵ -caprolactone	1	0.73	4	Full
P-LA-MA	D,L-lactide	2	0.71	4	Full
P-LG-MA	L-lactide	2	0.75	4	91%
	Glycolide	2	1.34	4	91%

^a Lactone feed ratios and calculated average block lengths are given in mole repeat units per mole hydroxyl groups on P-407.

^b Methacrylic anhydride (MA) feed ratio is given as mole MA per mole hydroxyl groups on P-407.

^c Conversion is shown as the percentage of hydroxyl groups converted to methacrylates.

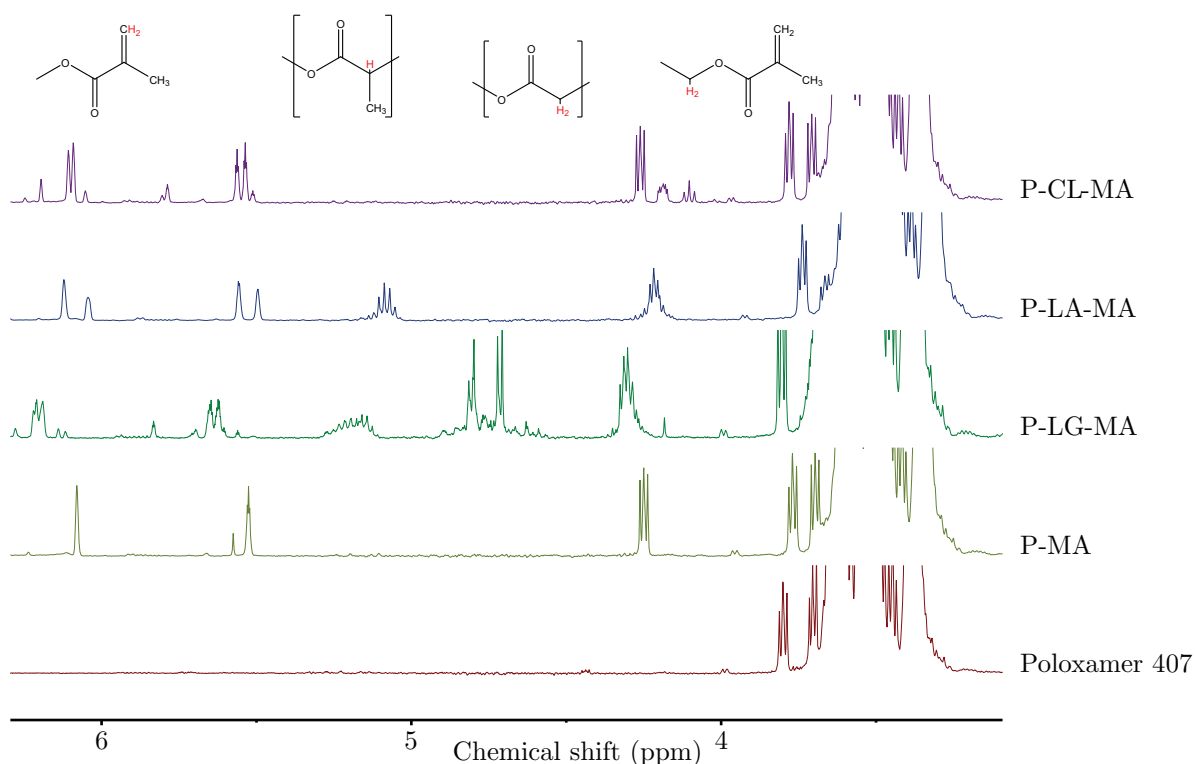


Figure S1. NMR spectra of the modified poloxamer macromonomers, compared to the NMR spectrum of unmodified poloxamer 407. Structural formulas are shown with protons in red over the range in the spectra where their peaks can be found. From left to right: protons from the vinyl group of methacrylate (5.5 and 6.0 ppm), single proton of lactyl (5.1 ppm), two protons of glycolyl (4.8 ppm) and protons adjacent to the terminal esters (4.3 ppm).

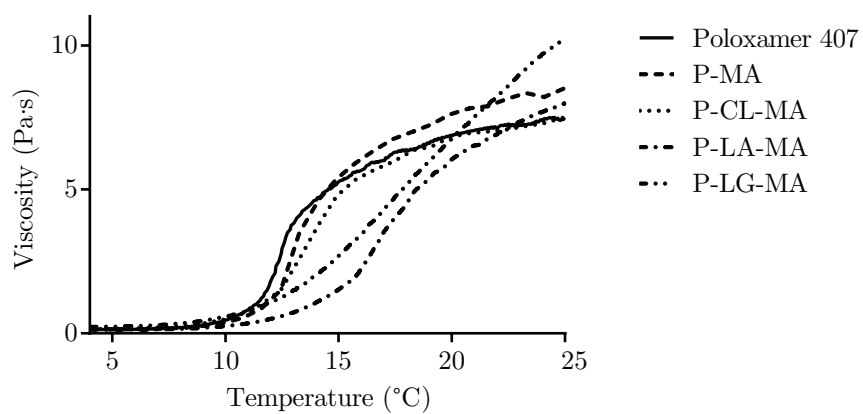


Figure S2. Viscosity measured as a function of increasing temperature from 4 to 25 °C for 28.6% gels based on modified and unmodified poloxamer. The applied shear rate was 100 s^{-1}